Economic Assessment of High-Thrust and Solar-Sail Propulsion for Near-Earth Asteroid Mining

Merel VERGAAIJ*[a], Colin R. McINNES†[a], Matteo CERIOTTI‡[a]

[a] *James Watt School of Engineering, University of Glasgow, G12 8QQ, Glasgow, United Kingdom*

Abstract

Asteroid mining has the potential to greatly reduce the cost of in-space manufacturing, production of propellant for space transportation and consumables for crewed spacecraft, compared to launching the required resources from the Earth's deep gravity well. This paper discusses the top-level mission architecture and trajectory design for these resource-return missions, comparing high-thrust trajectories with continuous low-thrust solar-sail trajectories. The paper focuses on maximizing the economic Net Present Value, which takes the time-cost of finance into account and therefore balances the returned resource mass and mission duration. The different propulsion methods are compared in terms of maximum economic return and sets of attainable target asteroids. Results for transporting resources to geostationary orbit show that the orbital parameter hyperspace of suitable target asteroids is considerably larger for solar sails, allowing for more flexibility in selecting potential target asteroids. Also, results show that the Net Present Value that can be realized is larger when employing solar sailing instead of chemical propulsion. In addition, it is demonstrated that a higher Net Present Value can be realized when transporting volatiles to the Lunar Gateway instead of geostationary orbit. The paper provides one more step towards making commercial asteroid mining an economically viable reality by integrating trajectory design, propulsion technology and economic modelling.

*Corresponding author, merel.vergaaij@glasgow.ac.uk
†colin.mcinnes@glasgow.ac.uk
‡matteo.ceriotti@glasgow.ac.uk

Keywords: Asteroid mining, trajectory optimization, Lambert arc, solar sail, Net Present Value

1. Introduction

For many years, science-fiction writers, space scientists and engineers have hypothesized about the potential advantages of asteroid mining (Lewis, 1996). However, due to technical, financial, and political challenges, commercial asteroid mining seemed to remain a distant fantasy (Gerlach, 2005). Nonetheless, the last few years have shown that asteroid mining is moving from a conceptual stage into a development stage, with a number of related companies emerging, aiming at commercial asteroid mining (European Space Agency, 2019; Meurisse and Carpenter, 2020; SpaceResources.lu, 2018). In the meantime, Earth-based observations and studies, combined with a number of missions to asteroids, have demonstrated that asteroids indeed contain vast quantities of valuable resources (Gerlach, 2005).

Easily-accessible key natural resources, upon which the development of many technologies are dependent, are in limited supply. Although humanity will not run out of easily-accessible critical raw materials for decades or even centuries to come, a point is reached where we can identify the limits of these resources (Gerlach, 2005). Furthermore, ambitious crewed interplanetary missions are planned (Salotti and Heidmann, 2014; International Space Exploration Coordination Group, 2018), as well as macro-scale structures in Earth orbit (Chmielewski and Jenkins, 2005), for which large quantities of space-based resources are required. Confronted with this, resources from space are becoming increasingly attractive and feasible options, particularly those from near-Earth space (Gerlach, 2005). Mining of natural resources from extraterrestrial sources, could provide a solution to the limited supplies of easily-accessible key natural resources on Earth and as building blocks for interplanetary exploration (Lewis, 1996; International Space Exploration Coordination Group, 2018). While lunar mining receives an increased amount of attention for near-term exploration

(International Space Exploration Coordination Group, 2018), this research focusses on exploiting near-Earth asteroids (NEAs), a number of which are more accessible than the Moon (Sonter, 1997).

Current work focuses on asteroid classification (Bus and Binzel, 2003), developing architectures and designing missions for asteroid mining (Andrews et al., 2015; Dorrington and Olsen, 2019), compiling sets of attainable target asteroids (Sanchez and McInnes, 2011; Yárnoz et al., 2013), trajectory optimization to NEAs (Tan et al., 2018; Peloni et al., 2016; Mingotti et al., 2014; Sánchez and Yárnoz, 2016), employing reusable launch vehicles (e.g., SpaceX BFR (Gargioni et al., 2019)) for asteroid mining missions or employing solar sails for sample return and mining missions (Dachwald and Seboldt, 2005; Hughes et al., 2006; McInnes, 2017; Peloni et al., 2016; Grundmann et al., 2019) and the economic modelling of asteroid mining ventures (Sonter, 1997; Ross, 2001; Hein et al., 2020; Gertsch and Gertsch, 2005; Andrews et al., 2015; Oxnevad, 1991; Dorrington and Olsen, 2019). While this addresses many issues important during the design of a profitable asteroid mining mission, little research has been done on integrating economical modelling into the optimization of trajectories to NEAs. This paper strives to address the gap between economic modelling and trajectory optimization, by integrating the two. Trajectory design which maximizes economic profitability will be investigated as a key consideration for future commercial ventures. Following related work on the economic modelling of asteroid mining (Sonter, 1997; Ross, 2001; Hein et al., 2020; Gertsch and Gertsch, 2005; Andrews et al., 2015; Bazzocchi and Emami, 2018; Oxnevad, 1991; Dorrington and Olsen, 2019), this work aims to maximize the Net Present Value (NPV) for a resource-return trip. The business case explored in this paper is built on returning volatiles (e.g., propellant) to geostationary orbit, where it can be used to refuel geostationary satellites or be stored in a depot for use in other orbits. The methodology can be applied to deliver (other) resources to other, potentially more profitable orbits, but the focus of this paper is to compare two different propulsion techniques and is therefore focused on the relative profitability of the transport element of asteroid mining missions.

Specific mining costs are not considered as the aim is to investigate the relative merits of chemical and solar-sail propulsion for resource transportation, trading off the benefits of solar sailing in reducing propellant mass with the impact on economics due to longer trip times.

The paper will investigate the maximum possible NPV for a single return trip to an asteroid and explore the region of Keplerian orbital elements of target asteroids for which the NPV can be positive. Rather than investigating the current family of 19,000+ NEAs [1], a grid of hypothetical NEAs is investigated, to indicate suitable regions of the parameter space for real target NEAs. To limit the dimensions of the grid, only semi-major axis, eccentricity and inclination are considered as parameters, leaving the remaining Keplerian orbital elements free in the optimization. This results in the maximum NPV possible for each given combination of semi-major axis, eccentricity and inclination. This analysis is carried out for both a high-thrust (chemical) mission scenario and a low-thrust (solar-sail) mission scenario. A genetic algorithm is employed to optimize Lambert arcs and solar-sail transfers, for the chemical and solar-sail mission, respectively, and additional parameters, such as the resource mass and the remaining Keplerian orbital elements of the hypothetical target asteroids.

To this extent, Section 2 lays out the mission architecture for both the chemical mission and the solar-sail mission. Then, Section 3 elaborates on the methodology for this work, including economic modelling and optimization of the transfers. Following this, Section 4 presents and discusses the results, after which the sensitivity analysis is presented in Section 5 and the paper is concluded in Section 6.

2. Mission architecture

A schematic for the proposed mission scenarios is presented in Fig. 1 for both the chemical and solar-sail mission. This paper focuses on the transportation

[1] JPL small-body database search engine, `https://ssd.jpl.nasa.gov/sbdb_query.cgi`, accessed on April 8th, 2019.

of mined resources and therefore it is assumed that the mining equipment has already been delivered to the asteroid, and that the resources are processed into LOX and LH_2. These scenarios can be summarized as follows:

- **Chemical propulsion**: launch to LEO (185 km) using the SpaceX BFR (Gargioni et al., 2019), which is used at its maximum allowable payload capacity (150 tons (Musk, 2018), i.e., 136 metric tonnes) with the cargo spacecraft and a kick stage, both including propellant. The kick stage will bring the cargo spacecraft from LEO to an escape trajectory with $C_3 = 0$ km^2/s^2. The cargo spacecraft will depart on a Lambert arc to the asteroid, where the mined and processed volatiles (LOX and LH_2) are waiting to be transported. A minimum stay time of one month is enforced to ensure enough time for rendezvous and docking. The resources are loaded into the propellant tanks of the cargo spacecraft which then departs on a Lambert arc to Earth using the asteroid-derived volatiles, where it will deliver the remaining resources to GEO at the end of the mission.

- **Solar sail:** launch to LEO (185 km) using the SpaceX BFR (Gargioni et al., 2019), which is again used at its maximum allowable payload capacity (136 metric tonnes (Musk, 2018)) with a fleet of mid-term solar sails (lightness number $\beta_0 = 0.1$ (Dachwald, 2005)) and a kick stage including propellant used to inject the stowed sails to an Earth escape trajectory with $C_3 = 0$ km^2/s^2. A fleet is used to ensure that the sails are of reasonable size, rather than one very large sail. After deployment at Earth escape, the sails spiral to the target asteroid, where the mined and processed volatiles (LOX and LH_2) are waiting to be transported. A minimum stay time of one month is again enforced to ensure enough time for rendezvous and docking. The resources are carried by the sails which then depart towards Earth, ending with a spiral from a parabolic approach to GEO where the resources are delivered.

Note that an investigation into the production rate of resources is considered outside the scope of this paper, and the time and effort for mining and pro-

cessing is not considered here. The reader is referred to the paper by Vergaaij et al. (2019) for a method to include the mining in this mission scenario. Also, it is assumed that the mission takes place in a mid- to far-term time frame, suggesting that intermediate missions have matured relevant technologies. The BFR has been chosen for these missions since it is assumed that the (promised) specific launch cost [$/kg] of the BFR ($96) is more likely to be the norm in a mid- to far-term timeframe, compared to the much higher specific cost for currently-available vehicles (∼$6-10k (Boone and Miller, 2016)).

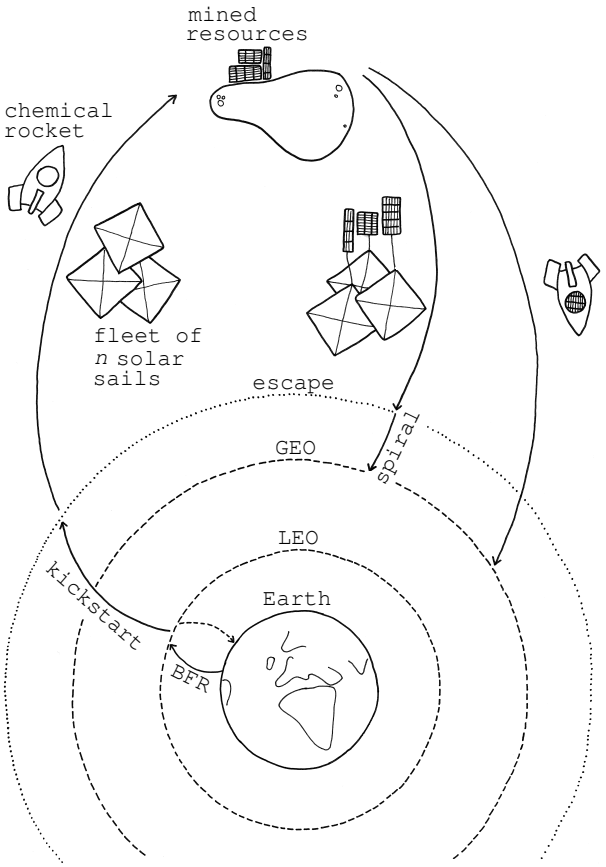

Figure 1: Schematic for both mission scenarios: using chemical transfers and solar-sail transfers.

3. Methodology

The goal of this paper is to find the maximum achievable economic return for a single return trip to a target asteroid for which the semi-major axis, eccentricity, and inclination are defined. A systematic grid search over these three Keplerian orbital elements will then yield the parameter hyperspace for which an asteroid mining venture can prove to be profitable.

To assess the economic viability of the asteroid mining mission concepts defined, the NPV has been adopted as a useful metric (Oxnevad, 1991; Sonter, 1997; Ross, 2001; Gerlach, 2005; Gertsch and Gertsch, 2005; Andrews et al., 2015; Hein et al., 2020; Bazzocchi and Emami, 2018; Dorrington and Olsen, 2018). Section 3.1 elaborates on the calculation of the NPV, which is the basis for the economic modelling. Subsequently, Sections 3.2 and 3.3 provide the optimization strategies to find the remaining orbital elements of the most ideally-placed target asteroids and the remaining parameters to define the missions, for the chemical mission and solar-sail mission, respectively.

3.1. Economic modelling

The NPV takes into account the forgone interest that the invested funds could have been earning: the longer the wait for income, the less present worth it has, and the more heavily discounted it must be (Ross, 2001). An NPV analysis uses costs and revenues over time and calculates the present value of the entire project (Oxnevad, 1991):

$$NPV = \frac{R}{(1+I)^{t_{mis}}} - C \tag{1}$$

in which R is the revenue, t_{mis} is the total mission duration in years, C is the incurred cost and the discount rate (I) is taken as 10% (Ross, 2001; Hein et al., 2020). Substituting for the cost contributions, this results in the following NPV

for the chemical propulsion mission:

$$
\begin{aligned}
NPV = \quad & \frac{p\left(m_{r,mined} - m_{r,used}\right)}{(1+I)^{t_{mis}}} \\
& -\left(C_{dev} + C_{man}\right) m_{s/c} \\
& -C_{prop} m^{O}_{prop} \\
& -C_{ks} - C_{l} - C_{op} t_{mis}
\end{aligned}
\tag{2}
$$

in which C_{dev} is the cost for development (per kg), C_{man} is the cost for manufacturing (per kg), C_{prop} is the cost for propellant (per kg), C_{ks} is the cost for the kick stage, C_l is the launch cost, C_{op} is the operation cost (per year) and p is the resource price to customers in GEO (per kg). Also, $m_{r,mined}$ is the total mined and processed resource mass to be transported to Earth (kg), $m_{r,used}$ is the resource mass used during the inbound transfer through in-situ resource utilization (kg), $m_{s/c}$ is the dry mass of the cargo spacecraft (kg), m^{O}_{prop} is the propellant used during the outbound transfer (kg) and t_{mis} is the total mission duration. All cost variables, as well as the derivation of the masses, are explained separately later in this section. The NPV for the solar-sail mission is similar:

$$
\begin{aligned}
NPV = \quad & \frac{p m_{r,mined}}{(1+I)^{t_{mis}}} \\
& -\left(C_{dev} + C_{man}\right) m_{sails} \\
& -C_{ks} - C_{l} - C_{op} t_{mis}
\end{aligned}
\tag{3}
$$

in which m_{sails} is the total mass of the fleet of solar sails (kg).

The Sections below summarize the methodology for obtaining the separate cost elements of the NPV calculation, with final data given in Table 1. Note that all costs have been corrected for inflation to FY2020 using NASA inflation tables (Hunt, 2018).

Sections 3.2 and 3.3 will elaborate on the remaining inputs for Eqs. (2) and (3), respectively.

3.1.1. Operation cost, C_{op}

The annual costs for operations are based on a robotic, low to moderately complex mission (Wertz et al., 2011). While it can be argued that the mission is more complex than this, the spacecraft will be in hibernation or an autonomous mode for most of the duration of the transfers. Moreover, the increased maturity of the technology in the mid- to far-term time frame can be considered.

3.1.2. Launch cost, C_l

The launch costs are for one fully reusable SpaceX BFR, for which the total cost is expected to be less than the cost of Falcon 1 (Musk, 2018). As a conservative estimate, the cost is assumed to be equal to the cost for the Falcon 1 vehicle (Wertz et al., 2011).

3.1.3. Development cost, C_{dev}

Conventional methods for determining the development and manufacturing costs are parametric cost models, analogy-based models, bottom-up models or process-based models. These methods all have to deal with limited data sets and the effects of rapidly changing technologies (Prince, 2015). They also rely on detailed information on the spacecraft and mission (e.g., mass, power, complexity, and/or a work breakdown structure). This level of detail is not available during concept development (Prince, 2015), especially in the case of "first-of-a-kind" or "state-of-the-art" missions (Lillie and Thompson, 2008). In addition, even if there were historical data analogous to the proposed asteroid mining mission (i.e., large space structures, interplanetary cargo systems, high-performance solar sails, and/or highly-autonomous robotics), historical data often suffers from a temporal, cultural, and technological gap due to time delay (Prince, 2003), causing inaccurate estimations. Therefore, another strategy for estimating the development and manufacturing cost has been explored.

Because of the complexity of accurately predicting the cost for spacecraft hardware, a specific cost based on mass is often employed, merely because it is the simplest to apply. Also, while mass may not be a cost driver, it is generally

a cost predictor (Prince, 2003). It is assumed that in a mid- to far-term time frame, the specific cost for space systems has decreased to the current specific cost for aviation systems. This is considered a fair assumption, since the current space sector increasingly resembles the history of aviation: growth of the space industry, commercialization, high production volumes (Pekkanen, 2019) and reusability (Musk, 2018).

Markish (2002) presents an overview of development and manufacturing cost per unit mass for each part of an aircraft and a fractional weight breakdown for a typical aircraft (in this case, a Boeing 777-200). A weighted average can be computed for the specific cost per kg. The non-recurring development cost consists of components for: engineering, manufacturing engineering, tool design, tool fabrication and support.

Also, in line with assuming aviation specific cost, aviation production volumes are also taken into account. Through May 2019, 2033 Boeing 777s have been ordered.[2] Since these costs are non-recurring, the development cost can be spread evenly over these units.

3.1.4. Manufacturing cost, C_{man}

Manufacturing costs are calculated as a weighted average according to data provided by Markish (2002). For manufacturing costs, the learning curve effect is also incorporated, which is characterized by a significant reduction in costs as additional units are built. The marginal manufacturing cost per unit, C_{man} after n units can be calculated using (Markish, 2002):

$$C_{man} = C_{man_0} n^{\frac{\log(b)}{\log(2)}} \tag{4}$$

in which C_{man_0} is the theoretical first unit cost and b is the learning curve slope. The learning curve slope used here is $b = 0.909$, which is a weighted average of labor (0.85), materials (0.95), and other (0.95) learning curve slopes (Markish, 2002).

[2] `http://www.boeing.com/commercial/#/orders-deliveries`, accessed May 31st, 2019

3.1.5. Propellant cost, C_{prop}

Costs for propellant are calculated for a LOX/LH2 engine, using standard prices for aerospace products reported by the Defense Logistics Agency (USA).[3]

3.1.6. Kick stage cost, C_{ks}

The cost for the kick stage is calculated in the same manner as the cost for other considered spacecraft, such that:

$$C_{ks} = (C_{dev} + C_{man})\, m_{ks} + C_{prop} m_{prop,ks} \tag{5}$$

where the mass for the kick stage (m_{ks}) is dependent on the required propellant mass ($m_{prop,ks}$). The propellant mass is calculated using the rocket equation:

$$m_{prop,ks} = m_l \left(1 - e^{-\frac{\Delta V_{LEO \to orbit}}{I_{sp} g_0}} \right) \tag{6}$$

where $m_l = 136$ metric tonnes is the launched wet mass, and $\Delta V_{LEO \to orbit}$ is the Hohmann ΔV to transfer from LEO to a target orbit. Then, using the minimum allowed structural coefficient, the kick stage dry mass is calculated:

$$m_{ks} = \frac{\epsilon_{min}}{1 - \epsilon_{min}} m_{prop,ks} \tag{7}$$

The minimum allowed structural coefficient (the mass of the structure divided by the mass of the structure and propellant) is assumed to be $\epsilon_{min} = 0.1$ throughout this paper (Sutton and Biblarz, 2010).

3.1.7. Resource price to customers in orbit, p

The price for which the resources are sold is dependent on the type of material to be sold (low value-to-mass or high value-to-mass) and where this material will be sold. If the material is to be sold in orbit, the price has to be competitive with the cost if the same material is launched from Earth. Kargel (1997) proposes that resources will be sold for a value p per kilo:

$$p = p' + C_{l,orbit} \tag{8}$$

[3] `https://www.dla.mil/Energy/Business/StandardPrices.aspx`, accessed May 31st, 2019

where p' is the cost of these materials purchased from terrestrial sources, in this case equal to C_{prop}, and $C_{l,orbit}$ is the launch cost per kg to the target orbit. For the sake of consistency, $C_{l,orbit}$ is calculated in the same manner as the cost for the missions discussed in this paper, and therefore includes a launch to LEO (185 km) using a fully loaded BFR and a kick stage to GEO (instead of escape). The total costs ($C_l + C_{ks,GEO}$) are then divided by the total mass delivered to GEO by the kick stage.

Table 1: Cost element inputs for NPV model.

Cost element	Value [FY2020 $]
C_{op}	6.98×10^6 /year
C_l	13.09×10^6
C_{dev}	37.19 /kg
C_{man}	1007.1 /kg
C_{prop}	0.95 /kg
p	488.08 /kg

3.2. Chemical mission scenario

To optimize the chemical mission for maximum NPV, the built-in genetic algorithm in MATLAB® is used to optimize the parameters below (Cage et al., 1994; Vasile et al., 2010). Note that, as explained in the introduction, the remaining free Keplerian orbital elements are optimized to find the most ideally placed hypothetical asteroid for a given semi-major axis, eccentricity and inclination, to return the maximum NPV possible in order to assess the region of orbital element space where the NPV can be positive. The parameters to be optimized are:

1. Duration of outbound transfer (Δt^O)
2. Stay time at target NEA (Δt_{stay})
3. Duration of inbound transfer (Δt^I)

4. Resource mass collected at target NEA in kg ($m_{r,mined}$)
5. Argument of periapsis of the target NEA (ω)
6. Right ascension of the ascending node of the target NEA (Ω)
7. Mean anomaly of the target NEA at t_0 (Jan 1, 2000, 11:58:55.816) (M_0)

These comprise the following decision vector for the genetic algorithm:

$$\mathbf{X} = \begin{bmatrix} \Delta t^O & \Delta t_{stay} & \Delta t^I & m_{r,mined} & \omega & \Omega & M_0 \end{bmatrix} \tag{9}$$

To aid convergence of the genetic algorithm and without constraining the optimization, this paper uses a combination of a fixed departure date for the inbound arc (Jan 1, 2024) in combination with transfer durations and a stay time, rather than absolute departure/arrival times. This eliminates the need for linear constraints (otherwise needed to ensure that the dates are chronological) and allows for smoother and faster convergence. Note that the mean anomaly of the target NEA at t_0 can be chosen to eliminate the effect of a fixed departure time.

The departure and arrival dates, in combination with the orbital elements of the Earth and the target NEA, lead to the states at departure and arrival, which subsequently lead to a ΔV for the associated Lambert arc: ΔV^O and ΔV^I for the outbound and inbound arc, respectively. Non-linear constraints are enforced to ensure that the minimum structural coefficient ($\epsilon_{min} = 0.1$, conforming to the requirement for the kick stage) is satisfied during both the outbound and inbound transfer, and that the resource mass is *at least* enough to bring the cargo spacecraft back to GEO.

The Lambert solver used in this work is written by Izzo (2015) in Python, but translated to MATLAB® to be used in conjunction with the genetic algorithm provided by MATLAB®. The dynamical model used is the Sun-centered two-body problem.

3.2.1. Bounds on parameters

Bounds on the parameters in Eq. 9 are defined in Table 2, including an explanation on the defined bounds.

Table 2: Bounds on parameters of decision vector of genetic algorithm for the optimization of the chemical mission.

Parameter	Minimum	Maximum	Explanation
Δt^O	30 days	max[2 years, $P_{hohmann}$]	In which $P_{hohmann}$ is the period of the Hohmann transfer orbit to the target NEA
Δt_{stay}	30 days	1 year	To allow time for docking and resource transfer
Δt^I	30 days	max[2 years, $P_{hohmann}$]	In which $P_{hohmann}$ is the period of the Hohmann transfer orbit to the target NEA
$m_{r,mined}$	0 kg	$514,234$ kg	Mass range allowed by the imposed constraints on the minimum structural coefficient
ω	0	2π	
Ω	0	2π	
M_0	0	2π	

3.2.2. Definition of remaining variables

The remaining variables for Eq. (2) are discussed below. The dry mass of the cargo spacecraft, $m_{s/c}$, is dependent on the propellant mass required for the outbound transfer, m^O_{prop}, together with the total mass injected into an escape orbit by the kick stage. First the wet mass of the cargo spacecraft ($m_{s/c,wet}$) is calculated:

$$m_{s/c,wet} = m_l - m_{ks} \tag{10}$$

then the propellant mass required to transfer to the asteroid is:

$$m^O_{prop} = m_{s/c,wet}\left(1 - e^{-\frac{\Delta V^O}{I_{sp} g_0}}\right) \tag{11}$$

and finally, the total dry spacecraft mass is:

$$m_{s/c} = m_{s/c,wet} - m_{prop}^{O} \tag{12}$$

Note that the chemical mission scenario makes use of in-situ resource utilization, so a fraction of the total mined resources ($m_{r,mined}$) is consumed during the inbound transfer:

$$m_{r,used} = \left(m_{s/c} + m_{r,mined}\right)\left(1 - e^{-\frac{(\Delta V^{I} + \Delta V_{capture \rightarrow GEO})}{I_{sp} g_0}}\right) \tag{13}$$

in which $\Delta V_{capture \rightarrow GEO}$ is the ΔV required to be captured at GEO from a parabolic return trajectory. The remaining mined resources will be sold upon arrival in GEO. The total mission duration t_{mis} is the difference between the departure time of the outbound transfer and the arrival time of the inbound transfer.

3.3. Solar-sail mission scenario

To optimize the solar sail mission scenario, MATLAB®'s built-in genetic algorithm is employed again, optimizing the same parameters as for the chemical mission scenario (Cage et al., 1994; Vasile et al., 2010; Vergaaij and Heiligers, 2019). However, the resource mass is not implemented as an absolute mass in kg, but as a (non-integer) multiple of the total sail mass (λ_r), allowing for faster constraint evaluation. This results in the following decision vector for the genetic algorithm:

$$\mathbf{X} = \begin{bmatrix} \Delta t^{O} & \Delta t_{stay} & \Delta t^{I} & \lambda_r & \omega & \Omega & M_0 \end{bmatrix} \tag{14}$$

Again, note that the departure and arrival dates, in combination with the orbital elements of the Earth and target NEA, lead to states at departure and arrival. To determine whether a solar sail transfer exist between the departure and arrival states for the given duration and sail performance, the solution to an optimal control problem should be sought. However, considering the high computational effort of solving an optimal control problem and the fine-tuning

of the solver necessary for each target NEA, this is infeasible for the scale of the problem at hand. Therefore, an alternative method is adopted, which has been chosen as a result of a trade-off between accuracy, computational effort and ease of implementation. This method will be detailed in Section 3.3.3.

3.3.1. Dynamical model

The dynamical model is again the two-body problem, but complemented with ideal solar-sail dynamics (McInnes, 1999, p.114):

$$\ddot{\mathbf{r}} = -\frac{\mu}{r^3}\hat{\mathbf{r}} + \beta\frac{\mu}{r^2}\left(\hat{\mathbf{r}}\cdot\hat{\mathbf{n}}\right)^2\hat{\mathbf{n}} \tag{15}$$

in which $\mathbf{r}$ is the position vector in Cartesian coordinates, μ is the gravitational parameter of the Sun, β is the sail lightness number, $\hat{\mathbf{n}}$ is the sail normal, which is defined in the radial-transverse-normal frame in terms of the cone angle, α, and the clock angle, δ. The cone angle is the angle between the incoming solar radiation and the sail normal, and the clock angle fixes the sail normal in three-dimensional space. Including a reference frame transformation to the inertial two-body frame, this is defined as (McInnes, 1999, p.115):

$$\hat{\mathbf{n}} = \begin{bmatrix} \hat{\mathbf{r}} & \hat{\mathbf{r}}\times\hat{\dot{\mathbf{r}}} & (\hat{\mathbf{r}}\times\hat{\dot{\mathbf{r}}})\times\hat{\mathbf{r}} \end{bmatrix} \begin{bmatrix} \cos(\alpha) \\ \sin(\alpha)\cos(\delta) \\ \sin(\alpha)\sin(\delta) \end{bmatrix} \tag{16}$$

3.3.2. Definition of remaining variables

The remaining variables for Eq. (3), where the NPV for a solar-sail mission is calculated, are discussed below.

During the outbound transfer, the lightness number is $\beta^O = \beta_0$. Upon collecting the mined resources at the asteroid, the lightness number of the sails for the inbound transfer decreases accordingly:

$$\beta^I = \beta_0\frac{1}{1+\lambda_r} \tag{17}$$

The last undefined variable in Eq. (3), t_{mis}, is a sum of the duration of both transfers, the stay time at the asteroid, and the time required to spiral from

a parabolic return trajectory to GEO. An analytical approximation is used to determine the time required for the spiral (McInnes, 1999, p.164):

$$t_{spiral} = \frac{2805 \text{ [days]}}{\beta^I \sqrt{r_{GEO}}} \tag{18}$$

3.3.3. Strategy to find feasible transfers

The method to determine whether a transfer is feasible, is based on the technique used by Vergaaij and Heiligers (2019). Using this method, an initial state is propagated forwards, and a final state is propagated backwards. Piecewise-constant controls are then optimized to minimize the discontinuity at the junction of the forward and backward phase. This paper uses the `fmincon` function from MATLAB® to determine four sets of constant controls (two to propagate forwards and two to propagate backwards). To increase the probability of `fmincon` converging to a solution, up to four different initial guesses can be used to initialize the optimization. For all four sets ($i = 1, 2, 3, 4$), these initial guesses are defined as follows:

$$\left[\alpha_i, \delta_i\right] = \left\{ \left[\alpha^*, 0\right], \left[\alpha^*, \tfrac{\pi}{2}\right], \left[\alpha^*, \pi\right], \left[\alpha^*, 3\tfrac{\pi}{2}\right] \right\} \tag{19}$$

i.e., for the first initial guess, *all four* sets of controls are $\left[\alpha^*, 0\right]$, for the second initial guess $\left[\alpha^*, \frac{\pi}{2}\right]$, etc. Furthermore, α^* is the cone angle which maximizes the force in the transverse direction of the sail (McInnes, 1999, p.118):

$$\tan \alpha^* = \frac{1}{\sqrt{2}} \tag{20}$$

The discontinuity in Cartesian coordinates (including both the position and velocity) at the junction of the forward- and backward-phase is calculated in non-dimensional units, where the unit of length is 1 AU, and the unit of time is 1 year. Using these non-dimensional units, a transfer is considered feasible if the norm of the discontinuity is less than 0.05. While the genetic algorithm, aiming to maximize the NPV, could exploit the maximum allowed discontinuity, previous work (Vergaaij and Heiligers, 2018, 2019) has shown that an optimal

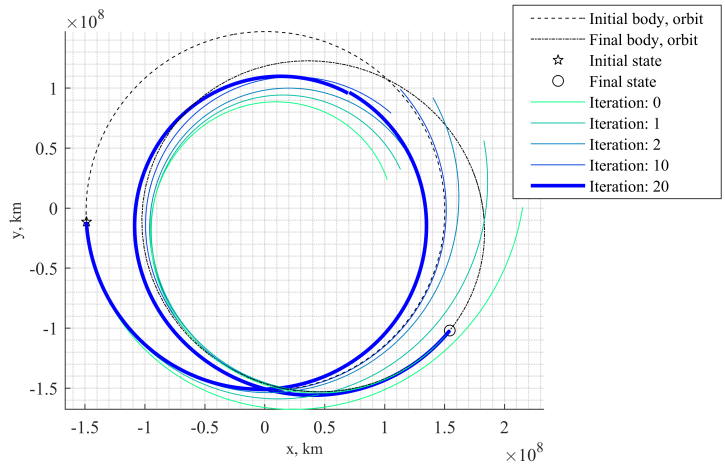

Figure 2: Example of the convergence of `fmincon` to a feasible transfer with a non-dimensional discontinuity of 0.04.

control solver is highly likely to be able to overcome a discontinuity of this magnitude. Also, note that this paper provides an initial investigation into the attainable targets. Once the target has been determined, a more high-fidelity approach can be used to optimize trajectories. Figure 2 shows an example of the iterations of `fmincon` to a feasible solution.

While this technique does not guarantee that minimum-time transfers are found, using a piecewise-constant control laws has shown to only cause a minor penalty on the transfer time, up to ∼4% (Mengali and Quarta, 2009).

3.3.4. Bounds on parameters

Bounds on the parameters defined in Section 3.3 are defined in Table 3, including an explanation for the defined bounds.

3.4. Pruning

The overall search area for target asteroids is based on the NEAs available in the Horizons database on March 6th, 2019 (Jet Propulsion Laboratory, 2019). An initial grid is placed between the minimum and maximum values of orbital elements in the Horizon database, with the semi-major axis and inclination

Table 3: Bounds on parameters of decision vector of genetic algorithm for the optimization of the solar-sail mission.

Parameter	Minimum	Maximum	Explanation
Δt^O	30 days	2 years	Based on extensive testing, any longer would result in a duration of the inbound transfer (far) exceeding the maximum bound.
Δt_{stay}	30 days	1 year	To allow time for docking and resource transfer
Δt^I	30 days	4 years	To limit the total duration of the mission, in order for the investment to remain attractive
λ_r	0	9	Consistent with $\epsilon_{min} = 0.1$
ω	0	2π	
Ω	0	2π	
M_0	0	2π	

constrained to 6×10^8 km and 42.5°, respectively, to remove outliers. A finer grid can subsequently be used to find the region of attainable target asteroids.

4. Results

Using the methodology described in Section 3, suitable regions of the parameter hyperspace have been determined for the mission architectures described in Section 2. The results for the chemical propulsion case are given in Section 4.1 and the results for the solar-sail case in Section 4.2.

4.1. Chemical propulsion

Figure 3 shows the maximum NPV for each node on the grid over semi-major axis, eccentricity and inclination. The combinations of these orbital elements which allowed for a positive NPV are circled in green, and those resulting in a

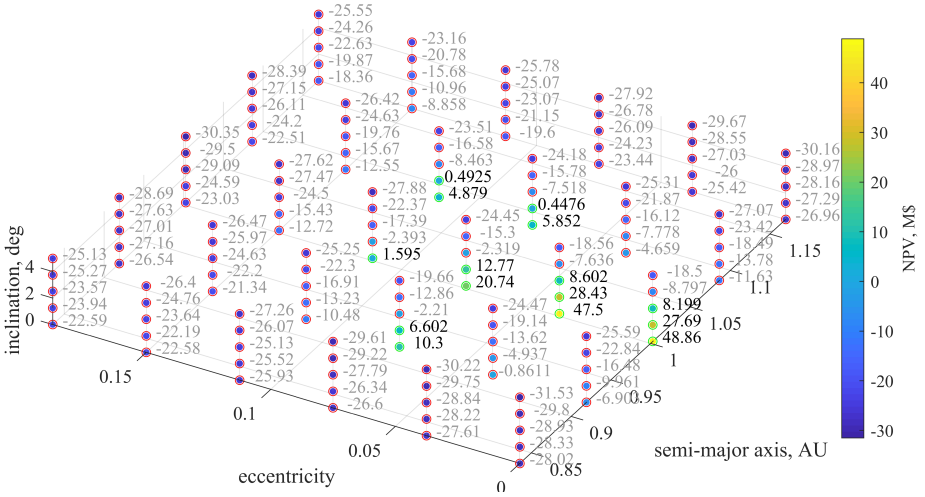

Figure 3: Maximum possible NPV (FY2020 million $) for each node on the grid for the chemical mission. Nodes for which a positive NPV is possible are circled in green, nodes for which only a negative NPV can be realized circled in red.

negative NPV are circled in red. Since Fig. 3 only shows the resulting NPV, a real asteroid from the Horizons system has been selected (based on the region of attainable targets) to perform the same analysis and show additional insight into a possible mission: NEA "2014 WX202". Note that in this case the remaining orbital elements are fixed and given by the Horizons system, and will therefore not be optimized. Instead, the departure date for the inbound transfer is added to the optimization, to allow for optimal timing of the transfers. The parameters resulting from the optimization for maximum NPV are given in Table 4. The results in Table 4 are merely given as an illustration of the data for a possible mission with a positive NPV, not to give the maximum NPV possible for all real target NEAs. The actual available volatile mass on the asteroid is not taken into account in the analysis.

4.2. Solar sail

Similar to the chemical propulsion case, Fig. 4 shows the maximum NPV for each node on the grid over semi-major axis, eccentricity and inclination for the solar-sail mission defined in Section 2. In addition, the details of an

Table 4: Example mission to NEA "2014 WX202" using chemical propulsion.

Parameter	**Value**	
Semi major axis	1.03564	AU
Eccentricity	0.05881	
Inclination	0.41270	°
Duration outbound transfer	238.6	days
Stay time at asteroid	30.0	days
Duration inbound transfer	276.2	days
$m_{r,mined}$	404,255	kg
ΔV^O (Lambert arc)	1.0525	km/s
ΔV^I (Lambert arc)	0.8909	km/s
m_l	136,078	kg
$m_{prop,ks}$	71,046	kg
m_{ks}	7,894	kg
$m_{s/c,wet}$	57,137	kg
m^O_{prop}	12,220	kg
$m_{s/c}$	44,917	kg
$m^I_{prop} = m_{r,used}$	175,324	kg
m_r to sell in GEO	228,932	kg
Launch cost	$ 13,095,922	
Development cost kick stage	$ 293,553	
Manufacturing cost kick stage	$ 7,954,986	
Propellant cost kick stage	$ 67,380	
Development cost spacecraft	$ 1,670,323	
Manufacturing cost spacecraft	$ 45,264,018	
Propellant cost spacecraft	$ 11,589	
Operations cost	$ 10,406,398	
Total cost	$ 78,764,171	
Revenue	$ 111,735,915	
Total mission duration	1.49	years
NPV	$ 18,162,380	

example mission to NEA "2006 RH120" are shown in Table 5 to gain insight into the relative cost of the different elements of the mission. Again, the results in Table 5 are given as an illustration of the data for a possible mission with a positive NPV, not to give the maximum NPV possible for all real target NEAs. Again, the actual available volatile mass on the asteroid is not taken into account.

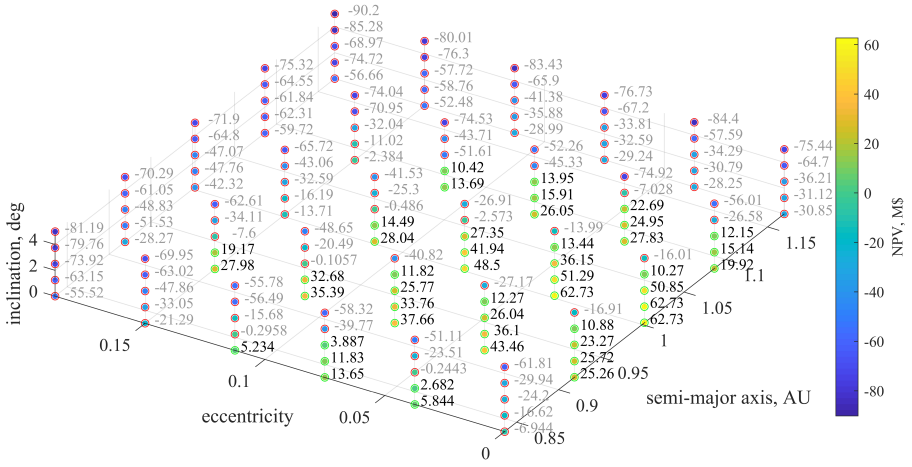

Figure 4: Maximum possible NPV (FY2020 million $) for each node on the grid for the solar sail mission. Nodes for which a positive NPV is possible are circled in green, nodes for which only a negative NPV can be realized circled in red.

4.3. Discussion

Suitable real target NEAs can be found in the regions resulting from Figs. 3 and 4, however, a positive NPV is not guaranteed: the combination of the remaining orbital elements is also important for the trajectory optimization to real target NEAs. In addition, the cost and effort for mining the resources has to be taken into account. However, the methodology presented here can be used however to prune the search space for future research.

Figure 3 shows a region of attainable targets for the chemical mission approximately between a semi-major axis of 0.9 and 1.1 AU, an eccentricity up to 0.1, and an inclination up to 2.5° (for more Earth-like target orbits, up to

Table 5: Example mission to NEA "2006 RH120" using solar sail propulsion.

Parameter	**Value**	
Semi major axis	1.00186	AU
Eccentricity	0.03513	
Inclination	1.08773	°
Duration outbound transfer	135.5	days
Stay time at asteroid	30	days
Duration inbound transfer	532.3	days
$m_{r,mined}$	514,234	kg
β^I	0.01	
Spiral time to GEO	1366.0	days
m_l	136,078	kg
$m_{prop,ks}$	71,046	kg
m_{ks}	7,894	kg
m_{sails}	57,137	kg
Launch cost	$ 13,095,922	
Development cost kick stage	$ 293,553	
Manufacturing cost kick stage	$ 7,954,986	
Propellant cost kick stage	$ 67,380	
Development cost spacecraft	$ 2,124,741	
Manufacturing cost spacecraft	$ 57,578,253	
Operations cost	$ 39,415,510	
Total cost	$ 120,530,345	
Revenue	$ 250,985,319	
Total mission duration	5.65	years
NPV	$ 25,944,319	

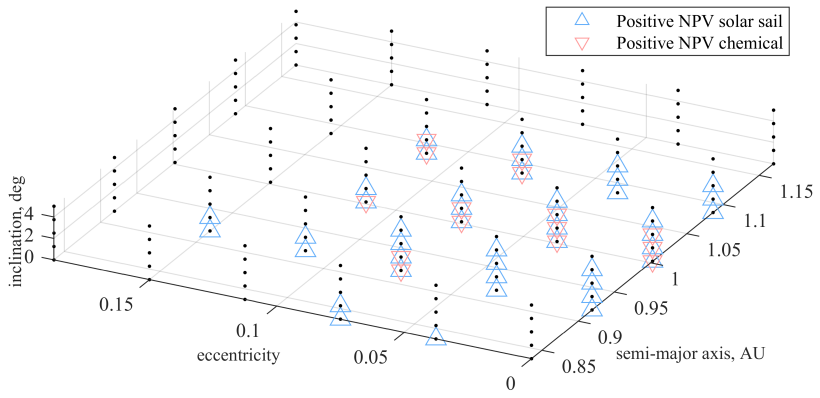

Figure 5: Comparison of attainable regions using chemical propulsion and solar sails.

1.25° for other target orbits). For more elliptical target orbits, the range of semi-major axes is larger than for more circular orbits. Similarly, Fig. 4 shows the region of attainable targets for the solar sail mission with semi-major axis between 0.85 and 1.1, eccentricity up to 0.15 and inclinations up to 3.75°. To properly compare the two regions, they are shown in the same plot in Fig. 5. It can be seen that the region of attainable targets is considerably larger for the solar sail mission than it is for the chemical mission. Even if the optimistic cost estimates do not materialize, this qualitative result is still valuable.

While the results presented here do not include the cost and effort for mining the resources, this can for example be included by bringing mining and processing equipment along to the asteroid (Vergaaij et al., 2019). Part of the launched mass will be dedicated to this equipment rather than the cargo spacecraft/sails, so less resources can be transported during the inbound transfer, causing a decrease in revenue for both the chemical and solar-sail mission. An equal decrease in revenue has a larger impact on the NPV for the chemical mission, because of the relatively smaller resource mass with respect to the solar-sail mission. In addition, time has to be spent at the asteroid to mine and process the resources, which influences the total mission duration and therefore the calculation of the discount in the NPV. An equal increase in mission duration would have a relatively larger effect on missions with an already longer duration: the solar-sail

mission. Future research will determine which effect is larger to determine the relative change in NPV for both cases. In absolute terms, the NPV will decrease for both missions, but Vergaaij et al. (2019) show that positive NPV can still be realized at least for the chemical mission. Also, in the case of a separate mining mission before the transportation mission, the increase in cost would be equal for both the chemical and solar-sail mission, causing an equal reduction in NPV. Comparing the difference in NPV between the two mission scenarios is then a measure for the relative benefits of chemical and solar-sail propulsion.

For the sake of comparison, the mission architecture in this paper assumes the same resources to be transported for both scenarios: volatiles. Transporting volatiles (or at least a fraction of the total resource mass) is critical for a chemical propulsion mission, due to in-situ resource utilization on the inbound transfer. The solar sail is not in any way constrained to which type of asteroid resource it transports, and could therefore also transport, for example, platinum group metals, which have a much higher value-to-mass ratio than volatiles. In contrast, a mission utilizing chemical propulsion needs to bring *at least* enough volatiles to return to Earth and only the remaining payload mass can be a type of resource with a higher value-to-mass ratio, such as platinum group metals or semi-conductors. In this case, multiple types of mining and processing equipment have to be used before the resources can be transported, and multiple types of containers are necessary. This is a disadvantage of using chemical propulsion instead of solar sails.

Another disadvantage of using chemical propulsion, is that due to in-situ resource utilization, a large fraction of the mined volatiles are consumed. While this paper assumes an infinitely large quantity of resource material available at the asteroid and costs for mining and processing operations are not considered in the analysis, in reality this is not the case. Mining and processing equipment has to be placed on an asteroid of finite size, and if a large fraction (e.g., 50%) of the processed resources never reach a customer, the mining and processing equipment has effectively only resulted in *half* the resources being delivered at the customer for the *full* cost. In contrast, solar sails do not consume propellant,

and are able to deliver the full payload to the customer, thereby leaving the total "value" of the asteroid and the mining and processing equipment intact.

Note that in this work it is assumed that all costs are incurred at the start of the mission, which in reality can be considered true for all costs except the operation costs. Costs incurred later would benefit from a higher discount, which is beneficial during the calculation of the NPV, especially for long duration missions.

5. Sensitivity analysis

This section provides three types of sensitivity analyses based on the results obtained in Section 4. First, the change in profitability of changing destinations from GEO to the Lunar Gateway is investigated. Second, a multi-trip mission is investigated and finally, a range of Monte Carlo simulations is presented.

5.1. Lunar Gateway

Another interesting location to sell volatiles is at or near the Lunar Gateway, where interplanetary spacecraft can refuel before or after interplanetary transfers (International Space Exploration Coordination Group, 2018). Changing the destination changes the propellant (m^I_{prop}) or spiral time for the inbound transfer, as well as the resource price (p). The location of the Lunar Gateway, at a halo orbit in the Earth-Moon system, is approximated energetically as being in a circular orbit at the lunar distance from the Earth. This requires the following substitutions: in Eq. (6) $\Delta V_{LEO \to Moon}$ is substituted for $\Delta V_{LEO \to orbit}$ to calculate the resource price p in Eq. (8), in Eq. (13) $\Delta V_{capture \to Moon}$ replaces $\Delta V_{capture \to GEO}$ to calculate the propellant required for the chemical return transfer, and in Eq. (18) r_{Moon} replaces r_{GEO} to calculate the spiral time for the sail.

Table 6 shows the optimized results for a single resource-return trip to the asteroid 2014 WX202 for the chemical mission and to asteroid 2006 RH120 for the solar-sail mission, for both the baseline result (GEO) and the Lunar

Gateway. The parameters not shown in these tables are the equal to those for the mission to GEO (and transfer durations within less than five days difference), as shown in Tables 4 and 5.

Table 6: Changed parameters for missions to the Lunar Gateway for both chemical propulsion (based on Table 4) and solar-sail propulsion (based on Table 5).

Parameter	**GEO**	**Lunar Gateway**	
$\Delta V_{LEO \to orbit}$ (to determine p)	3.940	3.968	km/s
p	\$ 488	493	
Chemical propulsion			
$\Delta V_{capture \to orbit}$	1.273	0.422	km/s
$m^I_{prop} = m_{r,used}$	175,324	117,265	kg
m_r to sell in GEO	228,932	289,939	kg
Revenue	\$ 111,735,915	142,983,745	
NPV	\$ 18,162,380	44,427,918	
Solar sail			
Spiral time capture to orbit	1366	452.4	days
Total mission duration	5.65	3.21	years
Operations cost	\$ 39,415,510	22,417,302	
Total cost	\$ 120,530,345	103,532,138	
Revenue	\$ 250,985,319	253,595,029	
NPV	\$ 25,944,319	83,157,309	

5.2. Multi-trip mission

While this paper focuses on single-trip missions, an approximation for a multi-trip mission can be calculated. For the chemical mission, an extension to the mission in Table 4 can be approximated by using $\Delta V_2^O = \Delta V^O + \Delta V_{GEO \to escape}$ in the analysis of the second trip. Furthermore, the mission duration as stated in Table 4 is doubled. This results in an increased operational cost, but the other costs are fixed. A fraction of the resources that were

to be sold in GEO are now used during the outbound transfer of the second trip, thereby reducing the profit of the first trip. The resulting NPV is then approximated as:

$$NPV = \frac{R_1 - C_{op_2}}{(1+I)^{t_{mis_1}}} + \frac{R_2}{(1+I)^{t_{mis_{1+2}}}} - C \tag{21}$$

where it is assumed that the increase in operation costs for the extended operations are paid at the start of the second leg. Naturally, other economic models for multi-trip missions are also possible. The results for this analysis are shown in Table 7. However, it should be noted that this analysis ignores the phasing of the second trip, which is likely to add a waiting period in GEO before the second leg commences.

Table 7: Extended mission to NEA "2014 WX202" using chemical propulsion.

Parameter	**Value**
Total duration 1st trip	544.8 days
ΔV_2^O	2.326 km/s
$m_{prop_2}^O$	31,530 kg
m_r left to sell 1st trip	194,213 kg
Total duration 2nd trip	544.8 days
Total cost 1st trip	$ 78,764,171
Cost extended operations	$ 10,406,398
Revenue 1st trip	$ 94,790,396
Revenue 2nd trip	$ 111,735,915
NPV	$ 78,515,665

One of the advantages of using a solar sail for transporting resources is that it can be reused, limited only by the lifetime of the sail. An extension to the mission in Table 5 can be approximated by including a spiral time from GEO to escape for the second trip (using Eq. (18)), and doubling the mission duration as stated in Table 5. This results in an increased operational cost, but the other

costs are fixed. The resulting NPV is then approximated as Eq. (21). The results of this analysis are shown in Table 8. Again, it should be noted that this analysis ignores the phasing of the second trip, which is likely to add a waiting period in GEO before the second leg commences.

Table 8: Extended mission to NEA "2006 RH120" using solar sail propulsion.

Parameter	**Value**
Total duration 1st trip	2063.8 days
Spiral time from GEO to escape	136.6 days
Total duration 2nd trip	2200.4 days
Total cost 1st trip	\$ 120,530,345
Cost extended operations	\$ 42,024,349
Revenue 1st trip	\$ 250,985,319
Revenue 2nd trip	\$ 250,985,319
NPV	\$ 83,909,035

As shown in Table 7, the spacecraft employing chemical propulsion can be used for a second trip to an asteroid. Even though the revenue of the second trip is discounted, it can be seen that a much higher NPV can be realized: \$78.5 million instead of \$18.2 million. Similarly, as shown in Table 8, a solar sail can be reused for a second trip to an asteroid. Again, the revenue of the second trip is heavily discounted, but much higher NPV can be realized: \$83.9 million instead of \$25.9 million. The long duration of the solar-sail mission means that the additional revenue suffers from a higher discount than is the case for the chemical propulsion mission, thereby not reaching the same multiplication of the NPV. However, the total mission duration could increase due to phasing in GEO, and the NPV realized using the multi-trip mission employing chemical propulsion would suffer relatively more from this increase in mission duration.

5.3. Monte-Carlo analysis

To investigate the sensitivity of the calculations with respect to the input values for the cost model, a range of Monte Carlo simulations have been performed. Separate simulations have been performed for the development cost (per kg), manufacturing cost (per kg), operation cost (per year), launch cost and discount rate, for both the chemical mission and the solar-sail mission to GEO. Uncertainties on the inputs, modelled using a standard deviation of 10% of the nominal value, lead to an uncertainty of the output value (NPV). Because the standard deviation is arbitrarily chosen and equal, the result is a relative metric for the sensitivity of certain input parameters with respect to the other parameters.

The results of the case studies as shown in Tables 4 and 5 are used as the baseline mission. For each simulation, 2000 scenarios are investigated, each changing only one input while leaving the others at the baseline. Because of the computationally-intensive nature of the optimization, the trajectories are not re-optimized, but the same trajectories for the baseline missions are used. This means that the resulting mission is likely suboptimal, resulting in slightly conservative values. The resulting histograms and fitted kernel probability density functions are shown in Fig. 6. These figures show that the assumed launch cost has a significant effect on the resulting NPV for propulsion techniques. For the solar-sail mission, which has a relatively long duration, the effect of the discount rate is more significant than it is for chemical propulsion.

6. Conclusion

In this paper, an approach has been presented to integrate economic modelling and trajectory optimization for asteroid mining ventures, employing either chemical propulsion or solar sailing. A grid of hypothetical NEAs (based on semi-major axis, eccentricity and inclination) is investigated, to indicate suitable regions of the parameter space for real target NEAs. The maximum possible NPV for a single-trip mission is investigated, which is launched by the SpaceX

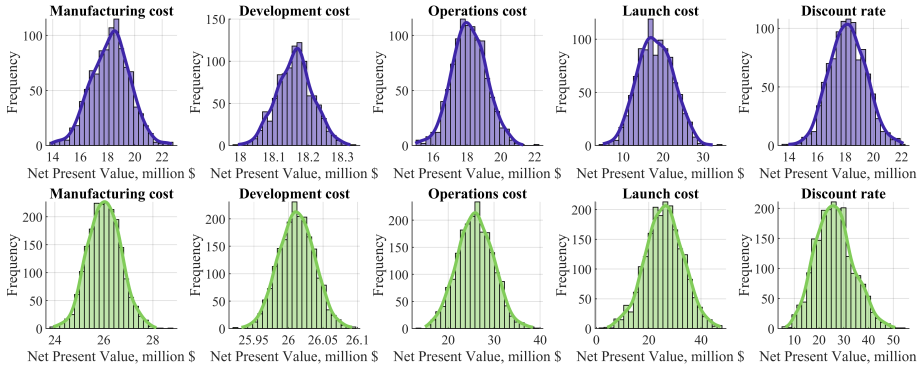

Figure 6: Result of Monte Carlo analyses, for both the chemical mission (top) and the solar-sail mission (bottom).

BFR and transports already-processed asteroid-derived volatiles to GEO, where the volatiles are sold at a price competitive with Earth launches.

Results show that for the mission scenario employing chemical propulsion, attainable targets have relatively Earth-like orbital elements; approximately a semi-major axis between 0.9 and 1.1 AU, an eccentricity up to 0.1 and up to 2.5° inclination (for Earth-like target orbits, up to 1.25° for other target orbits). The region for attainable targets is larger for a solar sail rather than chemical propulsion: semi-major axis between 0.85 and 1.1 AU, an eccentricity up to 0.15, and up to 3.75° inclination. It has been shown that for a chemical mission, values for the NPV up to $48.9 million are possible. Samples at the same grid nodes for a solar sail mission show values for the NPV up to $62.7 million. In addition, it is shown that increased values for the NPV can be realized if the resources are transported to the Lunar Gateway instead of GEO or if the mission includes a second trip to the same asteroid. A Monte Carlo analysis shows that the calculated NPV is sensitive to the launch cost assumed in the model, as well as a sensitivity to the discount rate, especially for long-duration solar-sail missions.

This paper therefore demonstrates that the region of attainable target asteroids (based on semi-major axis, eccentricity and inclination) is considerably larger for solar sail missions than it is for chemical propulsion, thereby allowing

more flexibility in selecting potential targets. While it should be noted that this mission scenario does not include the cost and effort required for mining the resources, the results still allow for a comparison of the two propulsion techniques. Likewise, if the optimistic cost estimates do not materialize, costs for both missions would increase, but this initial comparison will still hold. Besides the smaller region of attainable targets in the orbital element space, during the mission employing chemical propulsion a large fraction of the asteroid-derived volatiles is consumed, which decreases the total quantity of volatiles that can be delivered from a real target asteroid. These missions can also deliver non-volatile asteroid-derived resources to Earth orbit, such as platinum group metals or semi-conductors, which have a higher value-to-mass ratio than volatiles.

7. Acknowledgements

Merel Vergaaij gratefully acknowledges the College of Science and Engineering at the University of Glasgow for supporting this work, as well as Women in Aerospace - Europe and the Royal Aeronautical Society for support to attend the 5th International Symposium on Solar Sailing.

Colin R. McInnes was supported by a Royal Society Wolfson Research Merit Award and a Royal Academy of Engineering Chair in Emerging Technologies.

Matteo Ceriotti would like to thank the James Watt School of Engineering (University of Glasgow) and the Institution of Mechanical Engineers (IMechE Conference Grant EAC/KDF/OFFER/19/046) for supporting this work.

Bibliography

References

Andrews, D.G., Bonner, K., Butterworth, A., Calvert, H., Dagang, B., Dimond, K., Eckenroth, L., Erickson, J., Gilbertson, B., Gompertz, N., Igbinosun, O., Ip, T., Khan, B., Marquez, S., Neilson, N., Parker, C., Ransom, E., Reeve, B., Robinson, T., Rogers, M., Schuh, P., Tom, C., Wall, S., Watanabe, N.,

Yoo, C., 2015. Defining a successful commercial asteroid mining program. Acta Astronautica 108, 106–118. doi:10.1016/j.actaastro.2014.10.034.

Bazzocchi, M.C.F., Emami, M.R., 2018. Asteroid redirection mission evaluation using multiple landers. The Journal of the Astronautical Sciences 65, 183–204.

Boone, T.R., Miller, D.P., 2016. Capability and cost-effectiveness of launch vehicles. New Space 4, 168–189. doi:10.1089/space.2016.0011.

Bus, S., Binzel, R.P., 2003. Small Main-belt Asteroid Spectroscopic Survey, Phase II. Technical report. Planetary Science Institute. EAR-A-I0028-4-SBN0001/SMASSII-V1.0.

Cage, P., Kroo, I., Braun, R., 1994. Interplanetary trajectory optimization using a genetic algorithm, in: Astrodynamics Conference, American Institute of Aeronautics and Astronautics. doi:10.2514/6.1994-3773.

Chmielewski, A.B., Jenkins, C.H.M., 2005. Gossamer spacecraft, in: Jenkins, C. (Ed.), Compliant Structures in Nature and Engineering. WIT Press, Southampton, UK. volume 20, pp. 203–243. doi:10.2495/978-1-85312-941-4/10.

Dachwald, B., 2005. Optimal solar sail trajectories for missions to the outer Solar System. Journal of Guidance, Control, and Dynamics 28, 1187–1193.

Dachwald, B., Seboldt, W., 2005. Multiple near-Earth asteroid rendezvous and sample return using first generation solar sailcraft. Acta Astronautica 57, 864–875. doi:10.1016/j.actaastro.2005.04.012.

Dorrington, S., Olsen, J., 2018. Logistics problems in the design of an asteroid mining industry, in: 69th International Astronautical Congress (IAC), Bremen, Germany, 1-5 October 2018.

Dorrington, S., Olsen, J., 2019. A location-routing problem for the design of an asteroid mining supply chain network. Acta Astronautica 157, 350–373. doi:10.1016/j.actaastro.2018.08.040.

European Space Agency, 2019. ESA space resources strategy. pdf. URL: https://sci.esa.int/documents/34161/35992/1567260390250-ESA_Space_Resources_Strategy.pdf.

Gargioni, G., Alexandre, D., Peterson, M., Schroeder, K., 2019. Multiple asteroid retrieval mission from lunar orbital platform-gateway using reusable spacecrafts, in: 2019 IEEE Aerospace Conference, IEEE. doi:10.1109/aero.2019.8741985.

Gerlach, C.L., 2005. Profitably exploiting near-Earth object resources, in: 2005 International Space Development Conference, National Space Society, Washington, DC, May 19-22, 2005.

Gertsch, R., Gertsch, L., 2005. Economic analysis tools for mineral projects in space. Space Resources Roundtable .

Grundmann, J.T., Bauer, W., Biele, J., Boden, R., Ceriotti, M., Cordero, F., Dachwald, B., Dumont, E., Grimm, C.D., Herčík, D., Ho, T.M., Jahnke, R., Koch, A.D., Koncz, A., Krause, C., Lange, C., Lichtenheldt, R., Maiwald, V., Mikschl, T., Mikulz, E., Montenegro, S., Pelivan, I., Peloni, A., Quantius, D., Reershemius, S., Renger, T., Riemann, J., Ruffer, M., Sasaki, K., Schmitz, N., Seboldt, W., Seefeldt, P., Spietz, P., Spröwitz, T., Sznajder, M., Tardivel, S., Tóth, N., Wejmo, E., Wolff, F., Ziach, C., 2019. Capabilities of Gossamer-1 derived small spacecraft solar sails carrying Mascot-derived nanolanders for in-situ surveying of NEAs. Acta Astronautica 156, 330–362. doi:10.1016/j.actaastro.2018.03.019.

Hein, A.M., Matheson, R., Fries, D., 2020. A techno-economic analysis of asteroid mining. Acta Astronautica 168, 104–115. doi:10.1016/j.actaastro.2019.05.009.

Hughes, G.W., Macdonald, M., McInnes, C.R., Atzei, A., Falkner, P., 2006. Sample return from mercury and other terrestrial planets using solar sail propulsion. Journal of Spacecraft and Rockets 43, 828–835. doi:10.2514/1.15889.

Hunt, C., 2018. 2018 NASA new start inflation index. excel. URL: http://nasa.gov/sites/default/files/atoms/files/2018_nasa_new_start_inflation_index_for_fy19_use_final_dist.xlsx.

International Space Exploration Coordination Group, 2018. Global exploration roadmap. pdf. URL: https://go.nasa.gov/2nCkbFV.

Izzo, D., 2015. Revisiting Lambert's problem. Celestial Mechanics and Dynamical Astronomy 121, 1–15. doi:10.1007/s10569-014-9587-y.

Jet Propulsion Laboratory, 2019. JPL small-body database search engine. online, accessed on: April 8th, 2019. https://ssd.jpl.nasa.gov/sbdb_query.cgi.

Kargel, J.S., 1997. Semiconductor and precious-metal resources of metallic asteroids, in: Princeton Conference on Space Manufacturing, Space Studies Institute.

Lewis, J.S., 1996. Mining the sky. Addison-Wesley Publishing Company, Inc.

Lillie, C.F., Thompson, B.E., 2008. Parametric cost estimation for space science missions, in: Atad-Ettedgui, E., Lemke, D. (Eds.), Advanced Optical and Mechanical Technologies in Telescopes and Instrumentation, 2008, Marseille. doi:10.1117/12.789615. sPIE 7018.

Markish, J., 2002. Valuation Techniques for Commercial Aircraft Program Design. Phd thesis. Massachusetts Institute of Technology.

McInnes, C.R., 1999. Solar sailing: technology, dynamics and mission applications. Springer-Praxis series in space science and technology, Berlin. doi:10.1007/978-1-4471-3992-8_1.

McInnes, C.R., 2017. Harvesting near earth asteroid resources using solar sail technology, in: 4th International Symposium on Solar Sailing, Kyoto, Japan, 17-20 Jan 2017.

Mengali, G., Quarta, A.A., 2009. Solar sail trajectories with piecewise-constant steering laws. Aerospace Science and Technology 13, 431–441. doi:10.1016/j.ast.2009.06.007.

Meurisse, A., Carpenter, J., 2020. Past, present and future rationale for space resource utilisation. Planetary and Space Science 182, 104853. doi:10.1016/j.pss.2020.104853.

Mingotti, G., Sanchez, J.P., McInnes, C.R., 2014. Low energy, low-thrust capture of near Earth objects in the Sun-Earth and Earth-Moon restricted three-body systems, in: AIAA/AAS Astrodynamics Specialist Conference San Diego, CA, American Institute of Aeronautics and Astronautics. doi:10.2514/6.2014-4301.

Musk, E., 2018. Making life multi-planetary. New Space 6, 2–11. doi:10.1089/space.2018.29013.

Oxnevad, K.I., 1991. An investment analysis model for space mining ventures. International Transactions of the American Association of Cost Engineers .

Pekkanen, S.M., 2019. Governing the new space race. American Journal of International Law 113, 92–97. doi:10.1017/aju.2019.16.

Peloni, A., Ceriotti, M., Dachwald, B., 2016. Solar sail trajectory design for a multiple near-Earth asteroid rendezvous mission. Journal of Guidance, Control, and Dynamics, 39, 2712–2724. doi:10.2514/1.G000470.

Prince, F.A., 2003. Weight and the future of space flight hardware cost modeling, in: International Society of Parametric Analysis/Society of Cost Estimating and Analysis 2003 International Conference; 17-20 Jun. 2003; Orlando, FL; United States.

Prince, F.A., 2015. Why NASA's management doesn't believe the cost estimate. Engineering Management Journal 14, 7–12. doi:10.1080/10429247.2002.11415143.

Ross, S.D., 2001. Near-Earth Asteroid Mining. Space Industry Report. Control and Dynamical Systems, Caltech 107-81, Pasadena, CA 91125.

Salotti, J.M., Heidmann, R., 2014. Roadmap to a human Mars mission. Acta Astronautica 104, 558–564. doi:10.1016/j.actaastro.2014.06.038.

Sanchez, J.P., McInnes, C.R., 2011. Asteroid resource map for near-Earth space. Journal of Spacecraft and Rockets 48, 153–165. doi:10.2514/1.49851.

Sánchez, J.P., Yárnoz, D.G., 2016. Asteroid retrieval missions enabled by invariant manifold dynamics. Acta Astronautica 127, 667–677. doi:10.1016/j.actaastro.2016.05.034.

Sonter, M., 1997. The technical and economic feasibility of mining the near-earth asteroids. Acta Astronautica 41, 637–647. doi:10.1016/S0094-5765(98)00087-3.

SpaceResources.lu, 2018. Opportunities for Space Resources Utilization: Future Markets & Value Chains. Technical Report. Luxembourg Space Agency. URL: https://space-agency.public.lu/dam-assets/publications/2018/Study-Summary-of-the-Space-Resources-Value-Chain-Study.pdf.

Sutton, G.P., Biblarz, O., 2010. Rocket Propulsion Elements. 8 ed., John Wiley & Sons.

Tan, M., McInnes, C.R., Ceriotti, M., 2018. Low-energy near Earth asteroid capture using Earth flybys and aerobraking. Advances in Space Research 61, 2099–2115. doi:10.1016/j.asr.2018.01.027.

Vasile, M., Minisci, E., Locatelli, M., 2010. Analysis of some global optimization algorithms for space trajectory design. Journal of Spacecraft and Rockets 47, 334–344. doi:10.2514/1.45742.

Vergaaij, M., Heiligers, J., 2018. Time-optimal solar sail heteroclinic-like connections for an Earth-Mars cycler. Acta Astronautica 152, 474–485. doi:10.1016/j.actaastro.2018.08.008.

Vergaaij, M., Heiligers, J., 2019. Solar-sail trajectory design to planetary pole sitters. Journal of Guidance, Control, and Dynamics 42, 1402–1412. doi:10.2514/1.G003952.

Vergaaij, M., McInnes, C., Ceriotti, M., 2019. Influence of launcher cost and payload capacity on asteroid mining profitability. Journal of the British Interplanetary Society 72, 435–444.

Wertz, J.R., Everett, D.F., Puschell, J.J., 2011. Space Mission Engineering: The New SMAD. Microcosm Press, Hawthorne, CA.

Yárnoz, D.G., Sánchez, J.P., McInnes, C.R., 2013. Easily retrievable objects among the NEO population. Celestial Mechanics and Dynamical Astronomy 116, 367–388. doi:10.1007/s10569-013-9495-6.